Mathematical Model of a Constructal Coanda Effect Nozzle

M. Trancossi[1], J. Stewart[1], M. Subhash[2] and D. Angeli[3]

[1] *Faculty of Arts, Computing, Engineering and Sciences - Sheffield Hallam University, City Campus, Howard Street, Sheffield S1 1WB, UK*

[2] *Graphic Era University, 566/6 Bell Road, Clement Town, Dehradun-248002, India*

[3] *Di.S.M.I. - Università di Modena e Reggio Emilia - Pad. Morselli, Via Amendola, 2 Reggio Emilia, RE, 42122, Italy*

†*Corresponding Author Email: mtrancossi@gmail.com*

ABSTRACT

This paper analyses the ACHEON Coanda effect nozzle for aircraft propulsion, based on the dynamic equilibrium of two jet streams. The ACHEON concept, and, in particular, the HOMER nozzle, which is its main component, are presented, together with the literature milestones from which the idea originally stems. A subsystem analysis inspired by the principles of Constructal Theory is presented for the current architecture. A mathematical model of a 2D case of the system is developed, focusing on the combined effect of the mixing of the two streams and the Coanda adhesion over a convex surface. A validation of the model is also reported, based on 2D CFD analyses, under the hypothesis of incompressible flow. Results highlight that, in spite of its relative simplicity, the model produces accurate results.

NOMENCLATURE

A	area	x	length of adhesion
L	head losses		
p	pressure	α	angle
p_o	pressure on the curved surface	δ	boundary layer thickness
p_∞	external environment pressure	ν	kinematic viscosity
R, r	radius	θ	adhesion angle
Re	Reynolds number	μ	dynamic viscosity
t	outlet section thickness	ρ	density
u	tangential velocity of the flow	τ	wall shear stress
v	radial velocity of the flow		

1. INTRODUCTION

The EU FP7 project ACHEON (Aerial Coanda High Efficiency Orienting-jet Nozzle) presented by Trancossi and Dumas (2011a) proposes a novel propulsion concept which aims at producing a radically new aircraft propulsion system, with a potentially huge impact on the field of air transport. The concept comprises a thrust vectoring propulsive nozzle named HOMER (High-speed Orienting Momentum with Enhanced Reversibility), exploiting Coanda effect of a dual stream on a curved, convex surface, and a plasma actuator enabling the extension of the vectoring angle range of the nozzle. The integration of these two concepts involves both the way in which high speed streams mix and their interaction with Coanda surfaces, thus realizing a vectoring system, which can have a wide spectrum of applications. The optimization of the ACHEON system, and, in particular, of the HOMER nozzle requires the adoption of different means of analysis, such as velocity measurements and CFD. Nevertheless, the choice of the fundamental parameters and the assessment of optimum sets of their values, entail the definition of analytical integral models describing the operation of the system as a whole, and allowing for a convenient evaluation of the sensitivity of the system to geometrical features and boundary conditions. Furthermore, the use of macroscopic integral equations will be useful for the future defi-

nition of the guidelines for the operation and control of the system.

1.1 Constructal Theory

The Constructal theory (Bejan, 1997) is a logical model to tackle the description of natural phenomena and the optimization of engineering, logistic and management problems with a hierarchical approach. It is based on the Constructal principle enunciated by Bejan (1997): ''for a finite-size open system to persist in time (to survive) it must evolve in such a way that it provides easier and easier access to the currents that flow through it.'' Bejan (2006, 2010 and 2011) defined a logical flow path constructed by a sequence of blocks from elementary units to large system. The flow path is a sequence of steps that starts with the smallest building block (elemental block) and continues in time with larger building blocks (assemblies or constructs). The subsystem with the highest internal resistivity (slow flow, diffusions, walking, and high cost) has placed at the elemental block level, filling completely the lowest levels. Elements with successively lower resistivity (fast flow, streams, vehicles, and low cost) are placed in the larger constructs, where they connect the flow between elemental parts of the system. Using this network approach (Bejan 2008), the geometry of each building block can be optimized for its own specific functionality, thus leading to an optimum design of the overall construct.

Trancossi and Dumas (2011[b]) and (2013) took into account to the possibility of applying the Constructal principles to the modelling of the HOMER nozzle, which is a dual stream Coanda effect nozzle). A mathematical model of the nozzle has defined by subdividing the system into three different subparts, as Constructal theory suggests. Macro-scale models of the mixing process, as well as of the Coanda adhesion to a convex surface, and subsequent flow detachment are combined together to describe the overall process.

The model is then validated against preliminary CFD results, obtained by means of the ANSYS Fluent © software package. The simulations are performed under the assumption of 2D, incompressible flow. The comparison indicates that the simplified model predicts with a reasonable accuracy the detachment angle of the jet stream over the curved surface. Nevertheless, the slight discrepancies observed, and the preliminary nature of the evaluation leave space for further developments of the model.

1.2 Pioneering Models of Coanda Effect

A comprehensive bibliographic analysis on Coanda effect and Coanda nozzles has published by Trancossi (2011c), and integrated by Pascoa *et al.* (2013). Starting from this analysis it has been possible to produce an effective characterization of Coanda effect nozzles by their development and intrinsic properties, as a reference for the present work.

Different fluid dynamic effects concur to the determination of the so-called "Coanda effect", which has been defined by Coanda since 1910, although still in an embryonic formulation (Coanda 1936a). In particular, it has been formulated (Coanda 1936b) as the combination of three effects:

1. the tendency of a fluid jet approaching a curved surface to remain attached to the surface;

2. the adhesion effect, the ability of a fluid jet to adhere to a nearby surface; the attraction effect;

3. the tendency of jet flows over convex curved surfaces to attract surrounding fluid and expand more rapidly than that of plane wall jets.

A fundamental milestone characterizes the scientific studies about Coanda effect. Newman (1961) investigated two-dimensional, incompressible, turbulent jet flowing around a circular cylinder. The experiments by Newman involved a single stream and a cylindrical surface, with an experimental setup similar to the one schematized in Fig. 1.
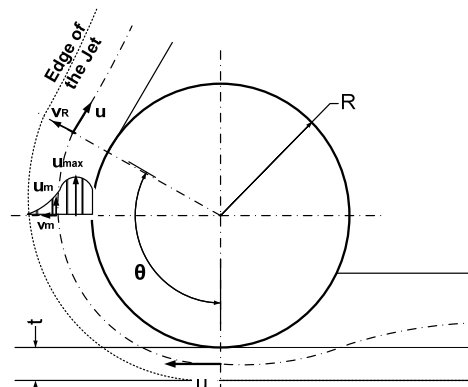

Fig. 1. Schematization of the Newman case study.

Newman demonstrated that Coanda adhesion to a curved convex surface is a direct consequence of the forces applied on the fluid. During adhesive motion on a curved wall, these are the centrifugal force and the radial pressure. As the jet goes out from the slot, the contact pressure with the curved wall is lower than the ambient pressure, because of the presence of viscous drag phenomena generated by the interaction of the fluid and the curved wall. This pressure differential is the main case of the fluid movement in contact with curved wall surface. The surface pressure along the curved wall rises and gradually equates the ambient pressure. In these conditions, there is a detachment between the curved wall and the fluid jet. Hence, the main geometric parameters of the system were the angle of separation θ, the slot width b, and the radius of curvature a, whilst the most relevant physical parameters were the Reynolds number Re and the pressure differential p_s-p_∞, (where p_s is the supply pressure). Using the setup schematized in Fig. 1, Newman obtained the following relation among the detachment angle θ_{sep} and the main geometric parameters and fluid dynamic quantities involved:

$$\theta_{sep} = f\left\{\left[\frac{(p_0 - p_\infty) \cdot t \cdot R}{\rho \cdot u^2}\right]^{0.5}\right\} \tag{1}$$

Bradshaw (1990) explained Coanda effect in terms of an inviscid irrotational flow and derived from the Bernoulli equation the formula:

$$p_0 - p_\infty < \frac{\rho \cdot u^2 \cdot t}{R} \tag{2}$$

where p_∞ is the external environment pressure. This expression is useful for an initial approach of a single jet Coanda adhesion. In real viscous flows the engagement of the fluid jet with a curved wall cause an increased jet thickness proceeding along the contact line, and a decrease of mean velocity, because of an adverse pressure gradient. Mean velocity decreases while surface pressure along the wall increases and eventually equals the ambient pressure. Postma, *et al*. (1973) demonstrated that the condition of detachment can be expressed as. by considering that the flow separates from the curved surface when $p_0 = p_{\infty}$. Therefore, inviscid flows may attach themselves according to the balance of centrifugal forces, but viscous effects are the cause for jet separation from the curved wall.

1.3 Boundary Effects and Detachment

Gorin (2008) have summarized development of the physical models for transfer processes in turbulent separated flows. He dedicated a particular attention to the factors that have allowed a better comprehension of the mechanism of transfer processes in separated flows, which differs from those in traditional attached turbulent flows in channels and zero pressure gradient turbulent flows. it is a fundamental issue for an accurate comprehension of the Coanda effect. Gorin assumes that the governing role of generated local pressure gradient that takes place in the immediate vicinity of the wall in separated flow is the result of intense instantaneous accelerations induced by large-scale vortex flow structures. He also introduces similarity laws for mean velocity and temperature profiles and spectral characteristics of the transfer processes.

Hasegawa (2008) analyses how boundary layer control can help avoiding flow separation problems on airfoils and in diffusers. The production of longitudinal (streamwise) vortices caused by the interaction between jets and a freestream using the vortex generator jet method it can be possible an effective separation, or stall control. This paper analyses how the active separation control system can be practically applied to the flow separation control of a two-dimensional diffuser. It was confirmed that the proposed active separation control system could adaptively suppress flow separation for the flow fields caused by some changes in freestream velocity and the divergence angle of the diffuser.

1.4 Enhanced Coanda Effect by Control jets

Many authors have discovered that high-speed jet streams blowing on the surface enhances Coanda adhesion. An effective system to produce an enhanced Coanda effect uses high-speed pilot jets, which enhance the adhesion to the surface. Such an architecture was defined by Postma *et al*. (1973), and Juvet (1993). Fig. 2 shows the general architecture of a system with pilot jets.

Juvet carried out an extensive testing using different blowing ratios with constant b/a = 0.031. The blowing ratio is defined as the ratio of the volumetric flow rate of the secondary flow to the flow rate of the primary flow. It was varied from 0 to 0.15, corresponding to a momentum ratio between 0.0 and 0.33. Notably, he found that a symmetric arrangement is not influenced by Coanda effect, regardless of the blowing through the secondary slot.
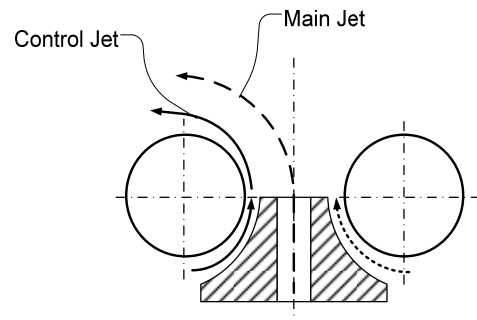

Fig. 2. Typical Coanda Nozzle with primary jet and control jets.

Other important conclusions were that:

1.   with blowing ratios below 0.1, the primary jet has a low influence by Coanda surfaces, and centreline velocity decreases due to entrainment of the secondary flow;

2.   with blowing ratios above 0.1 the main jet has been vectored in a radial direction and it has not any more the behaviour of a free jet.

3.   by increasing the blowing ratio the vectoring the vectoring capability increases.

Some interesting patents have also presented by Smith, forcing the typical Juvet architecture into three-dimensional architectures Smith (2007, 2010), exploiting a mechanically rotating pilot jet. These are also widely expressed by Allen (2007, 2008).

1.4 Enhanced Coanda Jets with Moving Surfaces

Many authors, especially in the field of aeronautic propulsion, have developed Coanda deflection systems based on moving surfaces and on pilot jet controlled applications with movable appendices. Wing (1994) focused on two-dimensional thrust vectoring of a primary jet using a secondary jet deflected via a Coanda surface (Fig.3). His experimental results

appear largely unsatisfactory, producing a maximum jet deflection about 6°. Wing concluded that the results have conditioned by a lack of momentum in the primary jet and that the nozzle design would require a best optimization to produce larger vectoring angles.

After some analysis it can be inferred that the disappointing results of the Wing experiments are strongly influenced by the nozzle design, which is largely borrowed by contemporary aircraft design.
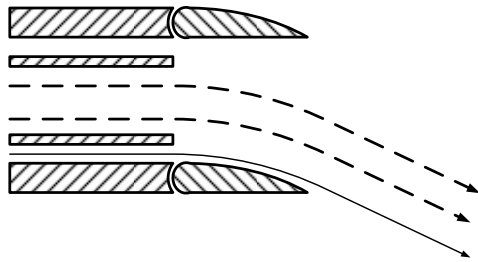

Fig. 3. Wing's experimental nozzle.

Mason (2002) reprised Wing's experimental studies using a similar experimental setup, and focusing his attention on the possibility of thrust vectoring by means of different geometries. Mason results presented vectoring angles better than those found by Wing, but the largest angle achieved was still relatively small (about 35°). Nonetheless, Mason's experiments assume a large importance because of the identification of three regions characterized by different momentum flow ratios:

1. dead zone: flow is sporadic and includes a negatively vectored occurrence;

2. control zone: vector angle versus momentum ratio or flow ratio can be assumed linear and can be controlled;

3. saturation zone: the vector angle no longer increases with increased momentum or flow ratio.

Mason's experiment constitutes the first attempt in creating a controllable Coanda jet-zone, and, to the author's knowledge, it is thus more related to the present study than any other further study.

1.5 Recent Applications of Coanda Adhesion

The flow over curved surfaces has ample applications in engineering such as the ones described by Freund (1994), Chang *et al.* (2009), Lee *et al.* (2007), Lalli, *et al.* (2010), Mabey *et al.* (2011), and Kim *et al.* (2006). In recent decades, the Coanda effect has been used in the design of the Rheolytic Thrombectomy devices, which proves its multidimensional applicability, which has been demonstrated by Chung *et al.* (2009). The water jet propulsion system by Mazumdar and Asada (2013) shows another important application.

Saghafi and Banazadeh (2009) consider again aeronautic propulsion uses and investigate the design

parameters for thrust vectoring. This is an important aid for other researchers to investigate the significance of these parameters. Because the parameters varies even with little modifications of the geometry, as verified by Subhash and Dumas (2013).

2. HOW ACHEON WORKS

The system architectures by Postma (1973) and Juvet (1993) have been the original inspirations for the ACHEON system and, in particular, for the HOMER nozzle. They present an architecture based on three streams, with one central main stream and two pilot jets, one in the lower part and one in the upper part. This architecture, even if very interesting, presents some limitation, especially concerning fast thrust direction changes in vectoring operations, such as the ones necessary for propulsion and aerodynamic control. Reducing the system to two high-speed jets only will largely simplify the equation of the system and the system control. This is the main reason that encouraged the initial study of the dual stream HOMER nozzle, as described by Trancossi and Dumas (2011, 2014).

This paper presents a model of the HOMER nozzle, which realizes two simultaneous operations: mixing two high-speed streams and Coanda effect adhesion. This problem has analyzed by applying Constructal Theory principles, dividing it in different elementary parts, which can be analyzed in sequence.

Fig. 4 represents a conceptual schema of the nozzle where 0 is the inlet section, 1 the mixing section, 2 is the actual nozzle outlet and 3 is the detachment section from the Coanda surface of radius R. The hypothesis of incompressible flow has assumed to hold for the time being.
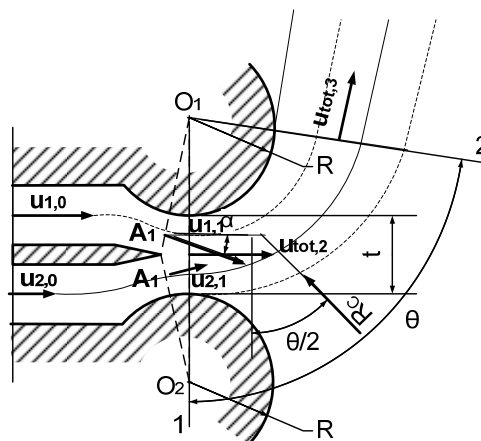

Fig. 4. Basic schema of the HOMER nozzle.

3. MATHEMATICAL MODEL

After the presentation of the architecture of the HOMER nozzle, it can be possible to define one of the possible mathematical models of the system. This model present is concurrent with the one presented by Trancossi *et al.* (2014) which has been defined by using integral equations and coupling

them with an exponential turbulence model. This model has worked accurately. Otherwise, it can be possible to define a second integral model starting by the intuition by Trancossi *et al* (2013). They have also used a integral equations, but assume the irrotational fluid motion hypothesis such as most of the authors from the aeronautic sector. This model allows producing an approximate description of the nozzle system.

The fluid domain has divided into different zones and specific equations have written to describe the behaviour of the system.

3.1 Inlet and Mixing Zone (0-2)

Referring to Fig. 4, conservation of mass writes:

$$u_{1,0}A_0 + u_{2,0}A_0 = u_{1,1}A_1 + u_{2,1}A_1 \qquad (3)$$

Furthermore, it is possible to express momentum conservation on two streamlines starting from inlet 1 and inlet 2. The mixing section 1-2 can be described assuming that the total area $2A_2$ is divided into two sections of area A_2:

$$u_{1,1}A_1 + u_{2,1}A_1 = \left(u_{2,1} + u_{2,2}\right)\cdot A_2 = u_{av,2}2A_2 \qquad (4)$$

$$p_{1,1} - p_{1,2} - L_{0,2} = \frac{1}{2}\rho\left[\left(\frac{A_2}{A_1}\right)^2 - 1\right]^2 u_{1,0} \qquad (5)$$

$$p_{2,0} - p_{2,2} - L_{0,2} = \frac{1}{2}\rho\left[\left(\frac{A_2}{A_0}\right)^2 - 1\right]^2 u_{2,0}^2 \qquad (6)$$

3.2 Adhesion Zone (2-3)

A possible approach to model the zone where the jet adheres to the Coanda surface could be to approximate the surface pressures induced on the curved surface wetted by the jet. However, a precise estimate would require the analysis of a wall-jet flowing over a convex surface with a non-uniform external flow field. This kind of analysis - as demonstrated by Roberts (1987) - presents non-trivial mathematical problems.

An approximate solution can start from the model by Bradshaw (1990). It is assumed that the streamlines due to Coanda adhesion are nearly circular and can be modelled as a potential flow, up to the point where the flow separates (3). This hypothesis is common in aeronautical engineering. Assuming two inlets, these will produce different velocities approaching the outlet, and the velocity profile in the outlet section is similar to the one represented in Fig. 5.

It can also been assumed that the real velocity profile due to the mixing effects changes its own shape reducing maximum velocity and increasing the minimum one, assuming a more regular profile and increasing the thickness of the boundary layer. The decay of velocity in the outer jet layer is modelled as a potential flow vortex. Fig. 6 shows an example of flow streamlines and velocity field induced by a circular vortex rotating around a point.
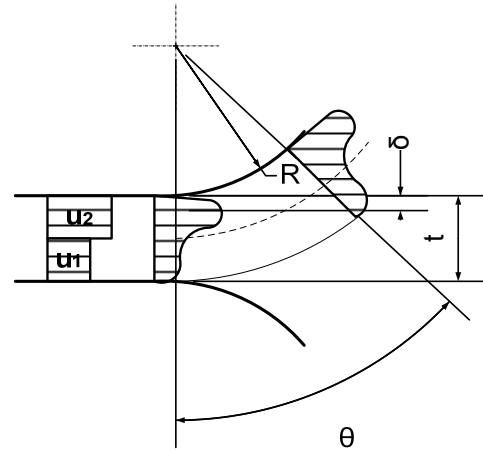

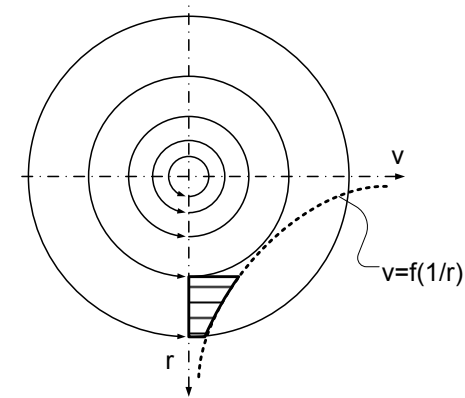**Fig. 5. Velocity profile hypothesis and evolution.**

Fig. 6. Streamlines and velocity profile produced by a circular vortex rotating around a point.

As demonstrated by various authors (Strykowski and Krothapalli 1993 and Davenport and Hunt 1975), the boundary layer is thin and gives a little contribution to the surface pressure, which has assumed constant across the boundary layer.

This simple model can be applied with a certain ease, without solving for the velocity of the entire flow field. It presents also a good agreement with the results presented by Davenport (1975), who demonstrated that circular streamline theory could provide reasonable estimates of the surface pressure. In particular, the system can be modelled using the simplified method presented by Keen and Mason (2005). They consider a Coanda flow in the case of a moving body neglecting the lower external speed, because of the hyperbolic velocity approximation of the speed in the vortex, and assuming Bernoulli's equation for incompressible flow, which can be expressed, if $u_{1,0}$ is greater than $u_{2,0}$, as:

$$p - p_\infty = -\frac{1}{2}\cdot\rho\cdot u^2 \qquad (7)$$

The proportionality of velocity with 1/r gives the following expression:

$$u_1(r) = u_{1,1}\frac{R}{r} \qquad (8)$$

which can be readily differentiated, thus giving:

$$\frac{d}{dr}u(r) = \frac{d}{dr}\left(u_{1,1}\frac{R}{r}\right) = u_{1,1}\cdot\frac{R}{r^2}. \tag{9}$$

It has verified that the proposed velocity models satisfy the potential flow condition. The following velocity limits has then theoretically considered in first approximation

$$u(r) \cong u_{1,1} \tag{10}$$

and

$$u(R+t) = u_{1,1}\frac{R}{R+t} \tag{11}$$

Assuming this velocity distribution on the inlet surface, one can evaluate how the velocity profile throughout the adhesion. Downstream the inlet, the external value of the pressure on the external surface of the stream will equal p_∞. The pressure has obtained by Eq. (7) which becomes

$$p_{w,2} - p_\infty = -\frac{1}{2}\cdot\rho\cdot u_{1,2}^2\cdot\frac{R^2}{(R+y)^2} \tag{12}$$

where $p_{w,2}$ represent the wall friction at the outlet. Differentiating in r, it results:

$$\frac{\partial p}{\partial r} = -\frac{1}{2}\rho\cdot u_{1,2}^2\cdot\frac{R^2}{r^3} = \frac{1}{2}\rho\cdot u_{1,2}^2\cdot\frac{R^2}{(R+y)^3} \tag{13}$$

By further integrating, the value of the pressure difference between the external and internal face can be calculated.

$$p_\infty - p_{wall} = -\frac{1}{2}\rho\cdot u_{1,2}^2\cdot R_{u_{max}}^2\left[\frac{1}{(R+y)^2} - \frac{1}{R^2}\right] \tag{14}$$

Despite the hyperbolic profile hypothesis, a more complex real velocity profile can be assumed, similar to the one. Taking into account the effect of the boundary layer the maximum velocity does not lay exactly on the circular surface but presents a different radius in real motion. This radius has been indicated as $R(u_{max})$. It can be calculated by Eq. (15):

$$R_{u_{max}} = \sqrt{2\cdot\frac{p_\infty - p_{wall}}{\rho\cdot u_{1,2}^2}\cdot\frac{R^2\cdot(R+t)^2}{(R+t)^2 - R^2}} \tag{15}$$

This value is always greater than *0* and describes the flux at the inlet. Considering the shear stress with the surface, even if it is neglected during calculations, it has been verified that

$$2\frac{p_\infty - p_{wall}}{\rho\cdot u_{1,2}^2} = 2\frac{\tau}{\rho\cdot u_{1,2}^2} = \frac{R_{(u_{max})}^2}{R}\left(1 - \frac{R^2}{(R+t)^2}\right) \tag{16}$$

where pressure in the detachment point is $p_3 = p_\infty$.

Assuming a third order polynomial velocity distribution in the boundary layer with the Coanda surface

$$\frac{u}{u_{1,2}} = \frac{3}{2}\frac{y}{\delta} - \frac{1}{2}\left(\frac{y}{\delta}\right)^3 = \frac{3}{2}\frac{r-R}{\delta} - \frac{1}{2}\left(\frac{r-R}{\delta}\right)^3 \tag{20}$$

it results

$$\tau = \mu\frac{du}{dr} = \frac{3}{2}\cdot\frac{u_{1,2}}{\delta}\cdot\left[1 - \frac{(r-R)^2}{\delta^2}\right] \tag{21}$$

The shear stress has evaluated as a function of velocity at $r=0$:

$$\tau = \mu\frac{du}{dr}\bigg|_0 = \frac{3}{2}\cdot\frac{u_{1,2}}{\delta} \tag{22}$$

Equalling Eqs. (17) and (19) one obtains:

$$\theta_{sep} = \frac{1}{3}\cdot\frac{\delta}{\nu}\cdot\frac{u_{1,2}}{R^2}\cdot\frac{(p_2 - p_3)R\cdot t}{\dfrac{\rho\cdot u_{1,2}^2}{2}} \tag{23}$$

Assuming:

$$\mathrm{Re}(\theta) = \frac{u_{1,2}R\theta}{\nu}$$

The thickness of the boundary layer is then evaluated:

1. for laminar flow:

$$\delta = 4.64\cdot\frac{x}{\sqrt{\mathrm{Re}(\theta)}} = 4.64\sqrt{\frac{x\cdot\mu}{\rho\cdot u}}$$

2. for turbulent flow:

$$\delta = 0.376\cdot\frac{x}{[\mathrm{Re}(\theta)]^{1/3}}$$

The above expressions can be generalized as follows

$$\delta = c\frac{R\theta}{\mathrm{Re}_\theta^{1/e}} = c\frac{R\theta}{\left(\dfrac{x\cdot\mu}{\rho\cdot u}\right)^{1/e}}$$

where e is a generic exponent.

and becomes

$$\delta = c\left(\frac{\nu}{u_{1/2}}\right)^{1/e}(R\theta)^{\frac{e-1}{e}} \tag{24}$$

Rearranging Eq. (23), the separation angle is then defined as:

$$\theta_{sep} = \frac{1}{(3\cdot c)^e}\cdot\frac{1}{\nu^{e-1}}\cdot u_{1,2}^{e-1}\cdot R\cdot\left(\frac{(p_2 - p_3)\cdot t}{\dfrac{\rho u_{1,2}^2}{2}}\right)^e \tag{25}$$

4. RESULTS AND DISCUSSION

The produced mathematical model appears simple and easy to be used and implemented. Even if it has considered one jet arrangement only, it is obviously

possible to describe the solution also when the jets invert their position.

The most relevant problem relates to the description of the fluid motion when the system is in the labile equilibrium case of identical velocity. In this case, one clearly obtains a deflection angle equal to zero.
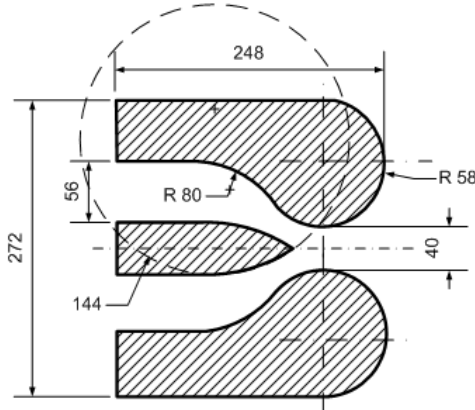

Fig 8. Geometry of the tested nozzle (units mm).

4.1 Preliminary CFD Validation

Numerical simulations have performed the validation of the results. The Spalart-Almaras turbulence models have been adopted according to Trancossi and Dumas. From bibliography, it seems reasonable suited for this kind of problems. The geometry used for the simulations is reported in Fig. 8. It is the same adopted by Trancossi and Dumas (2011b).

The simulations have been performed using the ANSYS Fluent ® CFD package. A simple triangular mesh was used, with a boundary layer refinement such as the one presented in Fig. 9 and 10. The convergence criteria was defined in terms of continuity residuals being lower than $1\,10^{-6}$. A validation has performed by adopting a young 2D product such as Easy CFD by University of Coimbra (Lopes 2010).

A detailed grid independence analysis of the cells near surfaces has performed by modifying the boundary layer thickness. The cells far from the walls of the nozzle has not been considered in this analysis because of their very low influence on the results has demonstrated in preceding literature (Trancossi and Dumas 2011, Subhash and Dumas 2013, and Trancossi *et al*. 2014).
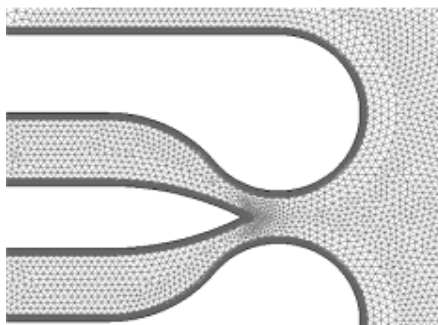

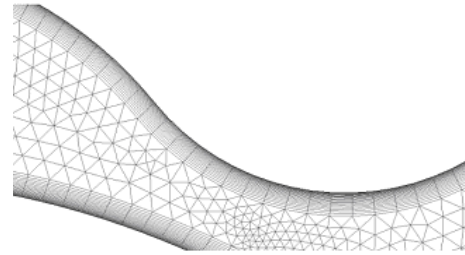**Fig. 9. Overview of the computational mesh.**

Fig. 10. Detail of the mesh.

The preliminary convergence computations has started with a Gambit/Fluent boundary layer grid of 5 mm (cell length) and initial thickness of 0.5 mm near the wall with a step increase of 1.1, 20 cells. It has been refined up to 1 mm with a step of 0.1 mm. The test case present a speed of 30m/s average and a individual speeds of the two fluxes v1 = 35 m/s and v2 = 25 m/s. The considered magnitudes are average velocity in the nozzle and adhesion length. The asymptotic behaviour has reached by a mesh with cell length of cells of 2.5 mm and thickness 0.25 mm with increase of 1.1 per step. It has then considered as the reference grid for further simulations.

4.2 Analysis of the Results

The analysis of velocity profiles at the nozzle outlet section shows that the hypothesis of a hyperbolic inlet velocity is reasonable, and that it becomes more and more effective with increasing the differences among the velocities. To this aim, a sample profile has been reported in Fig. 11. Different cases have been considered considering different stream velocities feeding the jet 1 and 2 (m/s). Sample pressure profile has also been reported in Fig. 12 considering different case with same average velocity u_{av}
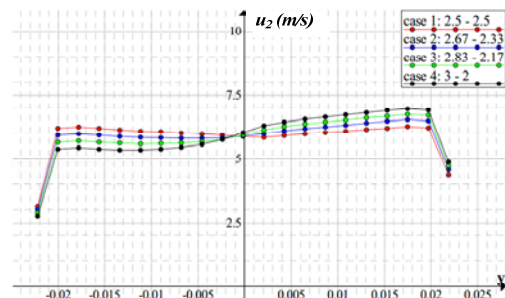

Fig. 11. Sample velocity profiles on section 2
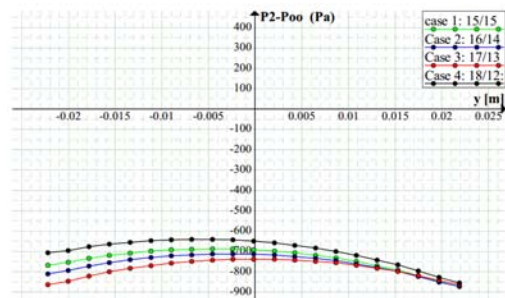($u_{av,0}$ = 2.5 m/s).

Fig. 12. Sample of pressure difference on section 2 ($u_{av,0}$ = 15 m/s).

The main parameters, which need to be evaluated for producing and effective verification of the results, are the angle of adhesion and the angle of the synthetic jet stream leaving the nozzle. It has been assumed that the the angle of adhesion and the angle of the jet are equal, according to the geometric scheme reported in Fig. 13.

This simplification does not consider that the trajectory of the stream changes from the ideal one and that the thickness and the geometrical section of the flux increases moving away along the Coanda surface.

Different cases were tested, with different velocity ratios. An example of the comparison between CFD and model results is reported in Fig. 14. For the calculation, Eq. (25) has been used, assuming p_1 and p_2 as the environment pressure minus the dynamic reduction of pressure due to the average velocities calculated according to the momentum equation in the mixing region. The outlet pressures p_1 and p_2 are obtained as average values in their half section at the end of the mixing area, as described above.
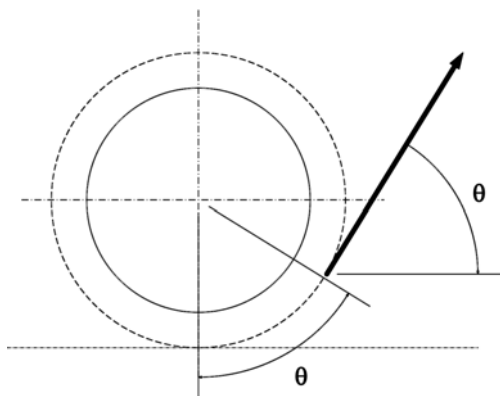

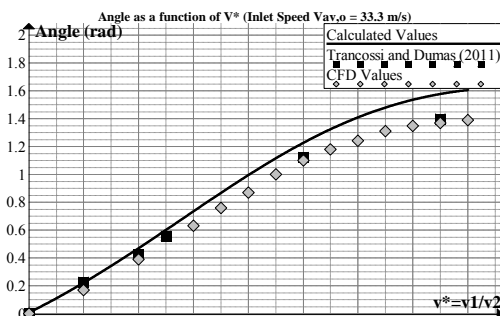**Fig. 13. Simplified calculation model.**

Fig. 14. Example of calculation with average inlet speed equal to 33.3 /ms.

Notwithstanding the approximate assumptions, results present a good agreement with CFD cases.

Similar results allows comparing calculation to the results presented by Trancossi and Dumas (2011b) and (2011c) on the same geometry but using an ideal gas model instead of the incompressible flow assumption adopted here.

The results suggest that the proposed method could be a reasonable basis for future development activities in the frame of the modelling of the control of a dual stream Coanda nozzle such as ACHEON. Moreover, the model is certainly acceptable for evaluating the Coanda Effect adhesion in the case of a synthetic jet.

However, some questions remain open. The first regards the evaluation of the pressures p_1 and p_2. They present some uncertainty in their calculation, which needs a deeper investigation more in depth. The second is linked with the relationship between effective adhesion angle and thrust direction, which requires a more detailed expression than the identity outlined in Fig. 13. It is also important to investigate the effects of the nozzle geometry on the calculated results to verify if they affect the errors of the model against CFD results.

5   CONCLUSION

An integral mathematical model, based on Constructal principles, has been developed for a dual stream, Coanda effect based nozzle for aeronautic application. The model relies on the subdivision of the system in three different subsystems, which are analyzed exclusively by theoretical means. The combination of the subsystem models provides an estimation of the jet deflection angle as a function of the inlet velocity ratio. A CFD validation of the model has been performed. A good correlation has found with data obtained by CFD, although the discrepancies suggest that the effect of friction is slightly underestimated.

REFERENCES

Allen D. S. and Smith B. L. (2007). Axisymmetric Coanda- assisted Vectoring. *submitted to Exp. Fluids, December.*

Allen, D. S. (2008*). Axisymmetric Coanda-Assisted Vectoring.* All Graduate Theses and Dissertations. Paper 90.

Bejan A. (1997). Advanced Engineering Thermodynamics, (2nd ed.). New York: Wiley.

Bejan A. and S. Lorente (2006). Constructal theory of generation of configuration in nature and engineering. *J. Appl. Phys. 100.*

Bejan A. and S. Lorente (2010). The Constructal law of design and evolution in nature. *Philosophical Transactions of the Royal Society B 365, 1335-1347.*

Bejan A. and S. Lorente (2011). The Constructal law and the evolution of design in nature. *Physics of Life Reviews 8, 209–240.*

Bejan A. and S. Lorente (2008). *Design with Constructal Theory*, Hoboken, Wiley.

Bradshaw, P. (1990). Effects of Streamline Curvature on Turbulent Flow. *AGARDograph AG-169.*

Celik, I., C. J. Chen, P. J. Roache and G. Scheurer (1993). Quantification of Uncertainty in Computational Fluid Dynamics. *ASME Fluids Engineering Division Summer Meeting 158, Washington, DC, 20-24 June.*

Celik, I. and O. Karatekin (1997), "Numerical Experiments on Application of Richardson Extrapolation With Nonuniform Grids. *ASME Journal of Fluid Engineering 119, 584-590.*

Chang, T. L., A. Rachman, H. M. Tsai and G. C. Zha (2009). Flow Control of an Airfoil via Injection and Suction. *Journal of Aircraft 46(1), 291-300.*

Chung, C. S., S. L. Cornejo, M. Huo and E. A. Finol (2009). A new concept in design of Rheolytic Thrombectomy devices. *Proc. ASME Summer Bioengineering Conference.*

Coanda, H. (1936a). US Patent n. 3,261,162, Lifting Device Coanda Effect, USA.

Coanda, H. (1936b). US Patent # 2,052,869, Device for Deflecting a Stream of Elastic Fluid Projected into an Elastic Fluid.

Davenport, F. J. and D. N. Hunt (1975). Deflection of a Thick Jet by a Convex Surface: A Practical Problem for Powered Lift. *AIAA Paper 75-0167.*

Eca, L. and M. Hoekstra (2002). An Evaluation of Verification Procedures for CFD Applications, *24th Symposium on Naval Hydrodynamics. Fukuoka, Japan, 8-13 July.*

Favre-Marinet, M., G. Binder and T. Hac (1981), Generation of oscillating jets. *Journal of Fluids Engineering 103, 609–614.*

Freitas, C. J. (1993). Journal of Fluids Engineering Editorial Policy Statement on the Control of Numerical Accuracy. *Journal of Fluids Engineering 115, 339-340.*

Freund J. B. and M. G. Mungal (1994). Drag and Wake Modification of Axisymmetric Bluff Bodies Using Coanda Blowing. *Journal of Aircraft, 31(3), 572-578.*

Gorin, A. (2008). Turbulent Separated Flows: Near-Wall Behavior and Heat and Mass Transfer. *Journal of Applied Fluid Mechanics 1(1), 71-77.*

Hasegawa, H. and S. Kumagai (2008). Adaptive Separation Control System Using Vortex Generator Jets for Time-Varying Flow. *Journal of Applied Fluid Mechanics 1(2), 9-16.*

Juvet, P. J. D. (1993). *Control of High Reynolds Number Round Jets.* Ph.D. thesis, Department of Mechanical Engineering, Stanford University.

Keen, E. B. and W. H. Mason (2005). A conceptual design methodology for predicting the aerodynamics of upper surface blowing on airfoils and wings. *Proc. 23rd AIAA Applied Aerodynamics Conference 6 - 9 June 2005, Toronto, Ontario Canada.*

Kim, H., G. Rajesh, T. Setoguchi and S. Matsuo (2006). Optimization study of a Coanda ejector. *Journal of Thermal Science 15(4), 331–336.*

Lalli, F., A. Bruschi, R. Lama, L. Liberti, S. Mandrone and V. Pesarino (2010). Coanda effects in coastal flows. *Coastal Engineering 57, 278-289*

Launder, B. E. and D. B. Spalding (1974). The numerical computation of turbulent flows. *International Journal for Numerical Methods in Fluids 15, 127-136.*

Lee, D. W., J. G. Hwang, Y. D. Kwon, S. B. Kwon, G. Y. Kim and D. E. Lee (2007). A study on the air knife flow with Coanda effect. *Journal of Mechanical Science and Technology 21, 2214-2220.*

Lopes, A. M. G. (2010). A versatile software tool for the numerical simulation of fluid flow and heat transfer in simple geometries. *Comput. Appl. Eng. Educ. 18, 14–27.*

Mabey, K., B. Smith, G. Whichard and T. McKechnie (2011). Coanda-assisted spray manipulation collar for a commercial plasma spray gun. *Journal of Thermal Spray Technology, 20(4), 782–790.*

Mason, M. S. and W. J. Crowther (2002). Fluidic Thrust Vectoring of Low Observable Aircraft. *CEAS Aerospace Aerodynamic Research Conference.*

Mazumdar, A. and H. H. Asada (2013). Pulse width modulation of water jet propulsion systems using high speed Coanda-effect valves. *J. Dyn. Sys., Meas., Control. 135(5), 051019-051019-11.*

Menter, F. R. (1997). Eddy viscosity transport equations and their relation to the k-ε model. *ASME Journal of Fluids Engineering 119, 876-884.*

Neuendorf, R. and I. Wygnanski (1999). On a turbulent wall jet flowing over a circular cylinder. *Journal of Fluid Mechanics 381, 1-25.*

Newman, B. G. (1961). The Deflexion of Plane Jets by Adjacent Boundaries, in Coanda Effect, in Boundary Layer and Flow Control , edited by G. V. Lachmann 1, 232–264.

Páscoa J. C., A. Dumas, M. Trancossi, P. Stewart and D. Vucinic (2013). A review of thrust-vectoring in support of a V/STOL non-moving mechanical propulsion system. *Central European Journal of Engineering.*

Postma A. K., J. D. Smith and D. S. Trent (1973). Development of a Concept for a High Capacity Pneumatic Conveying System Employing a Fluid Attachment Device for Use in Underground

Excavation, Final Technical Report, US Bureau of Mines.

Roberts, L. (1987). A Theory for Turbulent Curved Wall Jets. *AIAA Paper 87-0004*.

Saghafi, F. and A. Banazadeh (2009). Coanda surface geometry optimization for multi-directional co-flow fluidic thrust vectoring. *Proc. ASME. 48869; Microturbines and Small Turbomachinery; Oil and Gas Applications 5, 183-189.*

Shames, I. H. (2003). *Mechanics of fluids,* McGraw-Hill Higher Education.

Smith, B. L. (2007). High-speed jet control, United States Patent Application 20070158468.

Smith, B. L. (2010). High-speed jet control, United States Patent 7757966.

Strykowski, P. and A. Krothapalli (1993). *An experimental investigation of active control of thrust vectoring nozzle flow fields*, Tech. rep., The University of Minnesota.

Subhash, M. and A. Dumas (2013). Computational Study of Coanda Adhesion Over Curved Surface. *SAE International Journal of Aerospace, 6(1).*

Trancossi, M. and A. Dumas (2011 a). ACHEON: Aerial Coanda High Efficiency Orienting-Jet Nozzle. *Sae Technical Papers N.*

Trancossi, M. and A. Dumas (2011b). Coanda Synthetic Jet Deflection Apparatus And Control. *SAE Technical Papers N. 2011-01-2590.*

Trancossi, M. and A. Dumas (2011c). CFD Based Design Of A Nozzle Able To Control Angular Deflection, *Proc. ASME Int. Mechanical Engineering Congress And Exposition, Denver (CO), USA, Nov.*

Trancossi, M., A. Dumas, S. Das and J. Pascoa (2014). Design methods of Coanda effect nozzle with two streams. *Incas Bulletin Jan 2014, 83–95.*

Trancossi, M., M. Subhash and D. Angeli (2013). Mathematical modeling of a two stream Coanda effect Nozzle. *Proc. ASME Int. Mechanical Engineering Congress And Exposition 2013, San Diego (CA), USA.*

Trancossi, M. (2011). An Overview Of Scientific And Technical Literature On Coanda Effect Applied To Nozzles. *SAE Technical Papers N.*

Wilcox, D. (1994). Simulation of transition with a two-equation turbulence model. *AIAA Journal 32, 1192-1199.*

Wing, D. J. (1994). *Static Investigation of Two Fluidic Thrust- Vectoring Concepts on a Two- Dimensional Convergent- Divergent Nozzle.* Tech. Rept. NASA TM-4574, Hampton, VA.